



**Fermi National Accelerator Laboratory**

**FERMILAB-Conf-98/329**

**Beam Transport, Acceleration and Compression Studies in the  
Fermilab High-Brightness Photoinjector**

J.-P. Carneiro et al.

*Fermi National Accelerator Laboratory  
P.O. Box 500, Batavia, Illinois 60510*

October 1998

Presented at the *XIX International Linac Conference*,  
Chicago, Illinois, August 23-28, 1998

## **Disclaimer**

*This report was prepared as an account of work sponsored by an agency of the United States Government. Neither the United States Government nor any agency thereof, nor any of their employees, makes any warranty, expressed or implied, or assumes any legal liability or responsibility for the accuracy, completeness, or usefulness of any information, apparatus, product, or process disclosed, or represents that its use would not infringe privately owned rights. Reference herein to any specific commercial product, process, or service by trade name, trademark, manufacturer, or otherwise, does not necessarily constitute or imply its endorsement, recommendation, or favoring by the United States Government or any agency thereof. The views and opinions of authors expressed herein do not necessarily state or reflect those of the United States Government or any agency thereof.*

## **Distribution**

*Approved for public release; further dissemination unlimited.*

## **Copyright Notification**

*This manuscript has been authored by Universities Research Association, Inc. under contract No. DE-AC02-76CH03000 with the U.S. Department of Energy. The United States Government and the publisher, by accepting the article for publication, acknowledges that the United States Government retains a nonexclusive, paid-up, irrevocable, worldwide license to publish or reproduce the published form of this manuscript, or allow others to do so, for United States Government Purposes.*

# BEAM TRANSPORT, ACCELERATION AND COMPRESSION STUDIES IN THE FERMILAB HIGH-BRIGHTNESS PHOTOINJECTOR

J.-P. Carneiro, R. A. Carrigan, M. S. Champion, A. Cianchi, E. R. Colby, P. L. Colestock,  
H. T. Edwards, J. D. Fuerst, W. H. Hartung, K. P. Koepke, M. Kuchnir, L. K. Spentzouris  
Fermi National Accelerator Laboratory, Batavia, Illinois 60510 USA

M. J. Fitch, A. R. Fry, A. C. Melissinos, B. D. Taylor      P. Michelato, D. Sertore, C. Pagani  
Univ. of Rochester, Rochester, New York                      INFN-Milano-LASA, Milano, Italy

J. B. Rosenzweig  
University of California at Los Angeles, Los Angeles, Ca.

## Abstract

A photoinjector is being constructed in order to produce a pulse train of up to 800 electron bunches, each with 8 nC of charge and a 3.5 ps rms bunch length. The spacing between bunches within a train is 1  $\mu$ s and the train repetition rate is 1–10 Hz. The desired transverse emittance is  $<20\pi$  mm · mrad. An rf photo-gun delivers a bunched 4–5 MeV beam which will be accelerated to 14–18 MeV by a 9-cell superconducting cavity and compressed magnetically. Measurements have been done on the beam delivered by a first prototype rf gun; installation of a new rf gun, the 9-cell cavity, and the bunch compressor is in progress.

## 1 INTRODUCTION

A high-brightness electron source is being constructed at Fermilab as part of an ongoing collaboration with the TeSLA Test Facility (TTF) [1], and to provide an R&D facility for advanced accelerator research at Fermilab. The facility consists of a high quantum efficiency photocathode in a 1.3 GHz normal conducting rf gun, a 9-cell superconducting cavity for acceleration, and a magnetic bunch compressor (chicane). Thus far, an initial test with an rf gun has been completed. In particular, the important operational issues of dark current production and beam transport through the rf gun were studied. In this paper, we outline the results of the gun and beam studies thus far. When completed, the facility will be used to study beam transport through the cavity and the physics of compression with the high brightness beam. In the longer term, the facility will be used to explore a number of new acceleration schemes and to provide an R & D tool for a variety of new concepts relevant to high-energy, high-intensity machines, as will be described herein.

## 2 DESCRIPTION OF FACILITY

The beam line consists of a normal conducting rf gun, a superconducting acceleration cavity, a magnetic chicane, a low- $\beta$  section, a spectrometer, and diagnostics. In addition, there is a separate chamber for coating photo-cathodes and transferring them to the rf gun. The upstream portion of the beam line is shown in Fig. 1.

### 2.1 RF Gun

The rf gun consists of a 1.625-cell 1.3 GHz  $\pi$  mode copper cavity side-coupled to a waveguide in the full cell [2, 3].

The first prototype gun was intended for a low duty cycle ( $\sim 10^{-4}$ ). However, it was operated with a peak surface field on the cathode of  $E_c = 39$  MV/m with a pulse length of up to 400  $\mu$ s at a 1 Hz repetition rate; a 1 ms pulse was reached with  $E_c = 36$  MV/m at 0.1 Hz. The gun was used to produce beam at Argonne [2, 3] and Fermilab (see § 3).

A second generation gun has been designed for a high duty cycle (1%). The design parameters were (i) a beam energy of 3.9–5.5 MeV, which corresponds to  $E_c = 35$ –50 MV/m and a peak power dissipation of 2.2–4.5 MW; (ii) an rf pulse duration of 800  $\mu$ s; (iii) a repetition rate of 10 Hz. The high average power (up to 36 kW) is removed by cooling channels machined into the walls of the cavity, with  $\sim 4$  L/s of water flow. The first of the new guns has been fabricated and is presently being conditioned. To date, it has been operated with  $E_c = 40$  MV/m (2.7 MW peak power) with a 800  $\mu$ s pulse length at 1 Hz. Dark current measurements have also been done (see § 3.2).

### 2.2 Nine-cell Cavity

The superconducting accelerating cavity is a 9-cell structure made from sheet Nb [1]. Sub-systems include a high-power coaxial input coupler ( $Q_{ext} = 10^6$  to  $9 \cdot 10^6$ ), a cold tuner (range  $\approx \pm 400$  kHz), and 2 coaxial higher-order mode couplers. The current cavity, named S12, is a prototype fabricated by industry for TTF. It was etched, rinsed, heat treated, and tested with rf at DESY. The cavity is one of a batch with a low quench field (13 MeV/m in CW), attributed to contamination in the electron beam welds at the equator. The horizontal cryostat was designed at Orsay [4] for the TTF capture cavity and built by industry. After shipment to Fermilab, the cavity and cryostat were assembled, cooled to 1.8 K, and tested (without beam). With 800  $\mu$ s useful pulse length and 1 Hz repetition rate, the cryogenic load was tolerable at a gradient of  $\geq 12$  MeV/m. Further rf tests are needed to verify the field level calibration and measure the cryogenic losses versus field level.

### 2.3 Laser System

The ultra-violet (UV) laser for photo-electron production is a phase-stabilized mode-locked Nd:YLF oscillator ( $\lambda = 1054$  nm) and a chain of Nd:glass amplifiers, using chirped pulse amplification [5]. Seed pulses from the oscillator are stretched and chirped in an optical fiber, then selected by a fast Pockels cell (PC). A second fast PC is

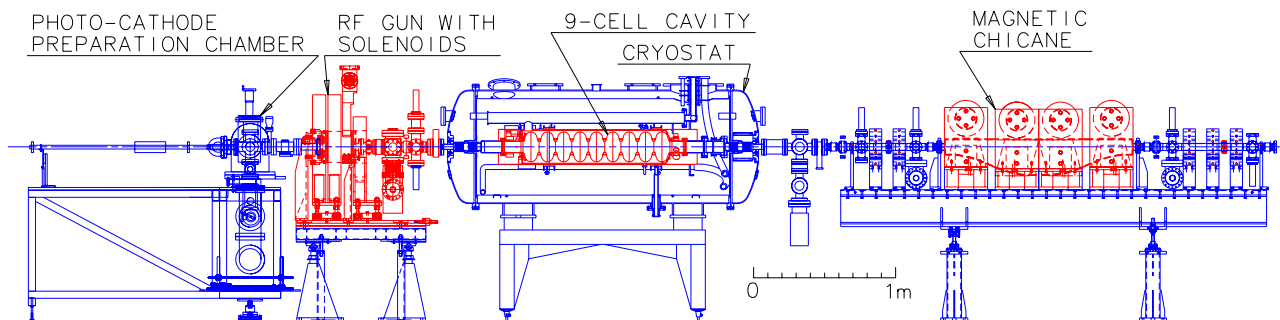


Figure 1. A0 beam line layout from the cathode preparation chamber through the chicane.

used to trap and eject the pulses into a multi-pass amplifier (see Fig. 2). After a 2-pass amplifier and spatial filtering, a grating compressor achieves a short, selectable pulse length (1–20 ps). Two stages of second harmonic generation are used to reach the UV wavelength (263 nm). The system is designed to produce  $5 \mu\text{J}$  per pulse of UV, in the following temporal pattern: pulse repetition rate of 1 MHz, pulses grouped into trains of 800, with 1 Hz repetition rate for the trains. The amplitude across the train is shaped via a third (slow) PC prior to amplification, to compensate for the time-dependent gain of the amplifiers, in order to produce a pulse train with a flat envelope.

## 2.4 Photo-cathode

The primary photo-cathode figure of merit is the quantum efficiency (QE), the ratio of the number of emitted electrons to the number of incident photons. The cathode is a  $\text{Cs}_2\text{Te}$  film on a Mo substrate.  $\text{Cs}_2\text{Te}$  can have a QE of up to 10–15%; for comparison, the QE of a metal cathode is typically  $10^{-4}$ – $10^{-6}$ . However, the QE of  $\text{Cs}_2\text{Te}$  is degraded by residual gases, so a  $\text{Cs}_2\text{Te}$  cathode must remain in ultra-high vacuum (UHV) for its entire useful life. A UHV system for coating cathodes and transferring them into the rf gun is hence required. So far, 2 cathodes have been coated and used with the first gun. For both, the QE was  $>10\%$  immediately after coating, about 0.6% after being used in the gun, and  $\geq 5\%$  after rejuvenation [6].

## 2.5 Diagnostics

The beam diagnostics include integrating current transformers (ICT), Faraday cups, beam position monitors (BPM), screens, emittance slits, and a magnetic spectrometer. The BPM's employ a heterodyne scheme to avoid rf noise and enhance signal strength. The screens are YAG, Cr-doped alumina, and Al, the latter being used for optical transition radiation (OTR) measurements with an intensified camera. The emittance slits consist of a rotatable array of 10  $\mu\text{m}$  slits approximately 20 mm high and 6 mm thick.

# 3 BEAM OPERATION

A first round of experiments was done at Argonne with the low duty cycle gun, a Cu cathode, and a Cu 9-cell cavity [2, 3]. A second round of experiments was done at Fermilab with the same gun (after retrofit for a  $\text{Cs}_2\text{Te}$  cathode), without a 9-cell cavity, as will be described in this section. The next step will be further experiments with the new high

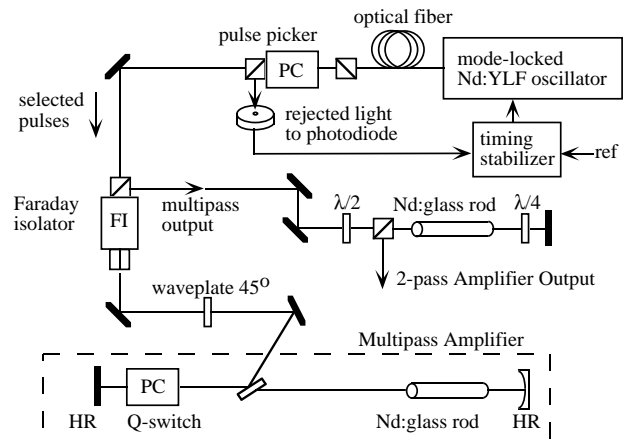


Figure 2. Block diagram of the laser system through the 2-pass amplifier.

duty cycle gun, 9-cell superconducting cavity, and chicane.

## 3.1 Photo-Current Measurements

Photo-electrons have been produced in pulse trains up to 50  $\mu\text{s}$  long, as shown in Fig. 3. At present, the limit on train length is set by the laser. The maximum charge per bunch extracted from the cathode and accelerated by the gun was 30 nC, 15 nC, and  $\sim 1$  nC for trains of 1, 9 and 50 bunches, respectively.

The maximum beam energy measured with the spectrometer was 4.7 MeV, with a corresponding RMS energy spread of 5 to  $8 \cdot 10^{-3}$ . The normalized horizontal and vertical emittances were  $9\pi$  and  $7\pi$  mm · mrad, respectively, as measured via a quadrupole scan (with 10 bunches, 1.2 nC/bunch, 4.5 MeV).

A scan of rf phase shows the expected peak of transmitted current around the operating phase (Fig. 4). Direct measurements of jitter show the laser-rf jitter to be less than 10 ps, which is the limiting resolution of the measurement.

A preliminary round of measurements was done with the BPM's, ICT's, Faraday cups, and the OTR screen. Various problems were identified, e.g. amplitude modulation in the low-level rf system and inadequate alignment of the gun and focussing solenoids to the beam line.

## 3.2 Dark Current Measurements

A large amount of dark current was generated in the first rf gun after retrofit. Since field emission is strongly dependent on the rf field strength, one would expect that the dark

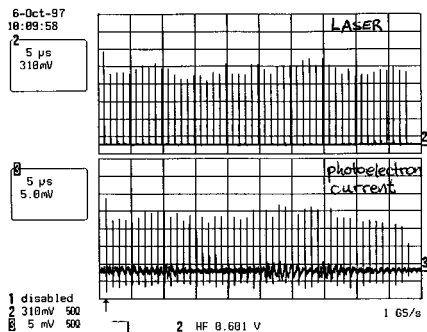


Figure 3. UV light incident on the cathode (top) and beam current (bottom) as a function of time ( $5 \mu\text{s}/\text{division}$ ). Vertical scales are uncalibrated.

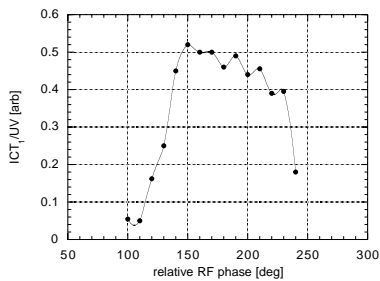


Figure 4. Normalized beam current versus rf phase.

current is generated at nearly full field, and thus emerges at full energy, but with a large energy spread. This was confirmed in spectrometric measurements. With the focussing solenoids set to image the emission on a screen downstream of the gun, it was inferred that the dark current was emitted primarily near the edge of the cathode, where a toroidal spring provides the rf contact between the cathode and the Cu wall of the gun.

In the second generation gun, the measured dark current is smaller by a factor of 20 at  $E_c = 38 \text{ MV/m}$ . We attribute this to careful cleaning procedures and to the use of a slightly different geometry and a new type of spring; however, the measurements on the second gun were made 0.2 m further downstream, which may account for some of the difference. Further tests on the new gun are underway.

## 4 PLANNED EXPERIMENTS

In addition to those described below, experiments are planned on the measurement of the longitudinal charge distribution of short bunches and on channelling acceleration.

### 4.1 Chicane Operation

In order to qualify the facility for future high-brightness applications, it is necessary to further compress the bunch length using a magnetic compressor, or chicane. While this procedure is routine, there are issues that need to be studied, including the effect of strong space charge forces on the transport through the chicane [7].

### 4.2 Plasma Accelerator Experiments

A key test of the plasma wake field accelerator (PWFA) [8] is planned among the first applications of this facility. Since the beam is of such high brightness, it provides an ex-

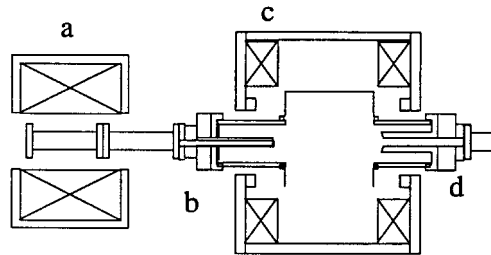


Figure 5. Plasma target chamber for PWFA, consisting of (a) matching solenoid, (b) cathode assembly, (c) plasma vessel with confinement solenoid, and (d) anode assembly. The plasma is generated between the 2 coaxial electrodes.

cellent driver of plasma waves in the PWFA, and should be the most definitive test of the achievable gradient to date. A plasma of  $1\text{--}3 \cdot 10^{13} \text{ cm}^{-3}$  is created in a target chamber located in a low- $\beta$  section of the beamline, shown in Fig. 5. Expectations are that gradients of  $1 \text{ GeV/m}$  should be achievable in this plasma.

## 5 CONCLUSIONS

A flexible, high-brightness photoinjector is under construction; it will provide an intense source of electrons for a variety of experiments. Initial experiments with a prototype rf gun have shown the expected beam properties, albeit accompanied by relatively large dark current. A second-generation gun has shown a promising reduction in dark current. Further work is now in progress to commission a chicane, and to optimize performance. Experiments on such concepts as the plasma wake field accelerator will commence in the near future.

## ACKNOWLEDGEMENTS

We thank our colleagues at Fermilab and in the TeSLA collaboration, especially S. Buhler, J. Crandall, R. H. Flora, T. Garvey, J. Gastebois, E. H. Hahn, M. Julliard, T. Junquera, T. W. Koeth, J. R. Le Duff, A. Matheisen, W.-D. Möller, W. Muranyi, F. A. Nezzrick, J. R. Noonan, M. J. Pekeler, P. S. Prieto, D. Reschke, J. K. Santucci, S. N. Simrock, J. J. Urban, M. M. White, and D. A. Wolff, for their participation in and many contributions to this project.

## REFERENCES

- [1] D. A. Edwards, Ed., “TeSLA Test Facility Linac—Design Report,” TeSLA 95-01, DESY (1995).
- [2] E. Colby, “A High Charge, High Duty Factor RF Photoinjector for the Next Generation Linear Collider,” these proceedings.
- [3] Eric R. Colby, Ph. D. Thesis, UCLA (1997).
- [4] S. Buhler et al., in *Proc. of the 7th Workshop on RF Superconductivity*, CEA/Saclay 96 080/1, p. 689–693 (1996).
- [5] Alan R. Fry, Ph. D. Thesis, University of Rochester (1996).
- [6] A. Fry et al., “Experience at Fermilab with High Quantum Efficiency Photo-Cathodes for RF Electron Guns,” these proceedings.
- [7] Bruce E. Carlsten, *Phys. Rev. E* **54**, p. 838–845 (1996).
- [8] J. Rosenzweig et al., “Proposal for Staged Plasma Wake-Field Accelerator Experiment at Fermilab,” P890 Proposal, Fermilab (1997).